Removal of Biocolloids Suspended in Reclaimed Wastewater by Injection into a Fractured Aquifer Model

CONSTANTINOS V. CHRYSIKOPOULOS,*,† COSTANTINO MASCIOPINTO,‡ ROSANNA LA MANTIA,‡ AND IOANNIS D. MANARIOTIS†

Environmental Engineering Laboratory, Department of Civil Engineering, University of Patras, Patras 26500, Greece, and Water Research Institute, National Research Council, Via Francesco De Blasio 5, 70123 Bari, Italy

Received September 11, 2009. Revised manuscript received November 21, 2009. Accepted December 5, 2009.

Two pilot-scale fractured aquifer models (FAMs) consisting of horizontal limestone slabs were employed to investigate the removal of biocolloids suspended in reclaimed wastewater. To better understand the behavior of real fractured aquifers, these FAMs intentionally were not "clean". The fracture apertures were randomly spread with soil deposits, and both FAMs were preflooded with reclaimed wastewater to simulate the field conditions of the Nardò fractured aquifer in the Salento area, Italy, where fractures are not clean due to artificial groundwater recharge. One of the FAMs was injected with secondary effluent from a wastewater treatment plant collected prior to the chlorination step and the other with exactly the same effluent, which was further treated in a commercial membrane reactor. Consequently, the organic and pathogen concentrations were considerably higher in the secondary effluent than in the membrane reactor effluent. Injected wastewater was continuously recirculated. Pathogen removal was greater for the secondary wastewater than the cleaner membrane reactor effluent. A simple mathematical model was developed to describe fracture clogging. The results suggest that the hydraulic conductivity of FAMs can be significantly degraded due to retention of viable and inactivated biocolloids suspended in reclaimed wastewater.

1. Introduction

Reclaimed wastewater is increasingly used worldwide for artificial groundwater recharge to reverse the rapid depletion of aquifers subject to growing demands for water and to inhibit saline intrusion in coastal aquifers (*1, 2*). Artificial groundwater recharge of reclaimed wastewater is accomplished by injecting recycled water into the subsurface (*3*−*6*). Important concerns associated with the usage of recycled water include the possibility of introducing infective human enteric viruses into groundwater systems (*7*) and clogging of the media (*8, 9*).

Groundwater contaminated by viruses has been detected at several reclaimed water recharge sites. Viruses are intracellular parasites with sizes ranging from 0.02 to 0.3 μm that can migrate along groundwater flowpaths; their transport and fate are significantly affected by virus inactivation and sorption onto the solid matrix (*5, 10*−*14*). However, virus transport is also affected by the water and soil chemistry (*15, 16*), the temperature (*5, 17*), and water saturation (*14, 18, 19*).

Biocolloid retention or removal in fractured and porous media leads to a reduction in void spaces and saturated hydraulic conductivity (*8, 20, 21*), which in turn contributes to a weak performance and possible clogging of artificially recharged aquifers (*9, 22*). Clogging is caused by a variety of interdependent mechanisms (physical, chemical, and biological), which may be different in fractured and porous media (*20, 23, 24*). Also, the degree of biocolloid removal is affected by several factors including biocolloid surface properties, fluid flow conditions, and physicochemical conditions of the formation (*6, 14, 19, 25*−*27*). Several mechanisms that lead to hydraulic permeability reduction of fractured and porous media have been studied at the laboratory (*20, 21*) and field (*9*) scale. Furthermore, various phenomenological, theoretical/analytical, and numerical mathematical models have been developed to describe clogging in porous media (*9, 28, 29*).

In this study we investigate the removal of pathogens from reclaimed water injected into a fractured aquifer model (FAM). The objectives of the work are to simulate the field conditions of the Nardò aquifer in southern Italy where the fractures are not "clean" and to monitor pathogen behavior during transport in a FAM. Pathogens are considered to be biocolloids that deposit onto fracture surfaces and can lead to hydraulic conductivity reduction and clogging of the FAM.

2. Experimental Apparatus

Each FAM employed in this study consisted of a closed PVC box with internal dimensions of 2.0 m length, 20 cm width, and 20 cm height. Inside the box were placed 16 limestone plates (slabs) with dimensions of 1.8 m length, 20 cm width, and 1.16 cm height (Fragassi Luigi Lavorazioni Marmi, Italy). The porosity of the limestone plates was 2.6%, as determined by quantitative relaxation tomography. A schematic representation of the FAM is shown in Figure 1. The limestone plates were previously treated with acid and chiseled to create rough surfaces. An adhesive rubber membrane was placed between the limestone plates and the side walls of the PVC box to prevent shortcuts of flow along the wall. Furthermore, the void spaces between the limestone plates (fracture apertures) were randomly spread with 2150 g of terra rossa soil deposits with a bulk density of 1.26 ± 0.1 g/cm^3 and low organic content (8−12 g/kg) to resemble the conditions found in the Nardò aquifer where the formation is fractured limestone intercalated by lenses of terra rossa with a mean fracture aperture of 1070 μm (*6, 30*). The terra rossa deposits consisted of 35−45% silica (quartz, feldspar, and calcite), 25−30% aluminum oxides (kaolinite and goethite), 10−15% iron oxides (hematite and magnetite), and trace amounts of calcium, potassium, titanium, magnesium, sodium, manganese, and phosphorus oxides (*31*). The initial porosity of the limestone parallel plate stack was volumetrically estimated to be 4.5% of the packed section. A 10 cm section at each end of the PVC box was kept unpacked to resemble a clear well.

Two sampling ports were placed in the effluent clear well. One sampling port was employed for continuous recircula-

* Corresponding author phone: +30 2610 996531; fax: +30 2610 996573; e-mail: gios@upatras.gr.
† University of Patras.
‡ National Research Council.

10.1021/es902754n
Published on Web 12/30/2009

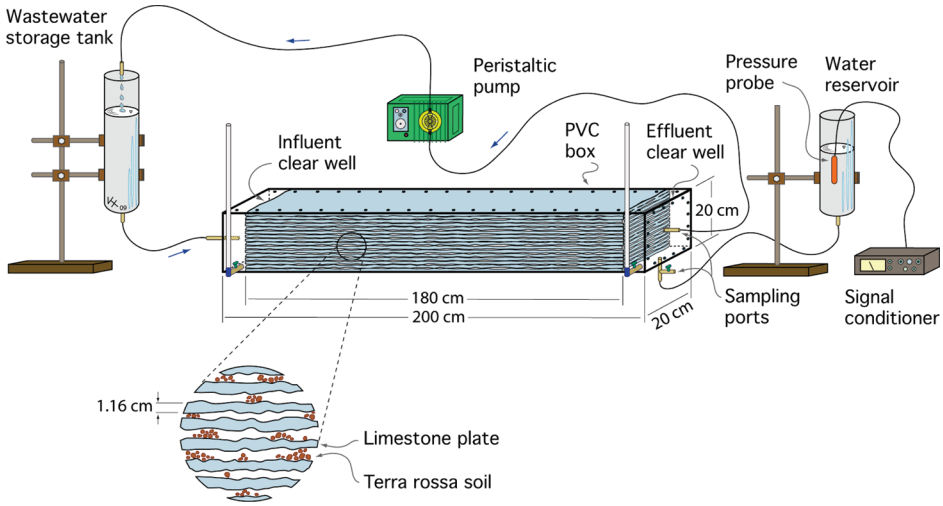

FIGURE 1. Schematic diagram of the experimental setup.

tion of the effluent with a variable-speed peristaltic pump (SEKO, Italy) back into the storage tank. The other sampling port was used for sample collection. A glass tube was attached to each of the two clear wells for visual observation of the hydraulic gradient. The piezometric head difference between the influent and effluent clear wells was measured with an electrical pressure probe having a precision of ±0.1 mm (PTX 164, Druck Ltd., England). The pressure probe was submerged into the water reservoir at the FAM outlet (see Figure 1). A probe reading of the reservoir head position was taken before the initiation of flow into the FAM. Subsequent probe readings indicated a decrease in head across the reservoir due to hydraulic head losses within the FAM. It should be noted that numerous other field (*32*) and laboratory (*33, 34*) experiments have used effluent stream recirculation.

A storage tank with a 35 L volume was used to feed wastewater into the FAM. The flow rate was controlled by a peristaltic pump. The wastewater was obtained from the Bari-West treatment plant in Bari, Italy. The wastewater was collected exactly prior to the chlorination step so that pathogens in suspension were not inactivated. The wastewater effluent was fed directly into FAM 1, while for FAM 2 the wastewater effluent was additionally treated by a laboratory-scale aerobic membrane-type reactor equipped with a Zenon Zee-Weed hollow fiber membrane module (nominal surface area 0.094 m^2 and pore size from 0.03 to 0.3 μm) operated at a negative pressure, which was maintained well below the limiting value suggested by the manufacturer (0.7 bar). The expected removal was 6−8 log for bacteria and 3−5 log for viruses.

3. Analytical Methods

A portion of the reclaimed wastewater was kept in a separate vessel (blank) to monitor the wastewater quality and to estimate inactivation rates of the pathogens present. The blank vessel was a 20 L plastic container, which was kept in the same room with the FAM. The FAM performance was evaluated by the systematic analysis of grab samples taken from the sampling port in the effluent clear well (see Figure 1). All samples were analyzed according to APHA Standard Methods procedures (*35*). The chemical oxygen demand (COD) and soluble COD (SCOD) were measured by the open reflux method (the alternate low-COD procedure was employed when appropriate). The total suspended solids (TSSs) were measured by drying at 103−105 °C and weighing the solids retained during filtration through a cellulose acetate membrane (0.45 μm pore size). The dissolved oxygen (DO) was measured with the membrane electrode method (WTW Oxi 340i, Germany). Furthermore, the electrical conductivity (EC), pH, total dissolved solids (TDSs), and temperature were measured with a multiparameter instrument (HI 991301, Hanna Instruments). The initial quality characteristics of the reclaimed wastewater together with the operational parameters of each FAM are listed in Table 1.

TABLE 1. Operational Parameters and Wastewater Quality Characteristics of the Two FAMs

param	FAM 1	FAM 2
Q_w (L/d)	120 ± 7.6	104 ± 11.8
T (°C)	18.4 ± 0.54	18.3 ± 0.52
pH	7.39−7.75	7.40−7.71
DO (mg/L)	0.2−0.9	1.9−4.1
EC (mS/cm)	3.38 ± 0.09	3.58 ± 0.09
TDSs (ppt)	1.69 ± 0.04	1.82 ± 0.02
COD (mg/L)	72 ± 14	30 ± 7
SCOD (mg/L)	44 ± 8	28 ± 5
TSSs (mg/L)	20 ± 9	<2
ρ_b (mg/cm^3)	1.022	1.066
$\bar{b}$ (mm)	1.08	1.23
$K(t = 0\ d)^a$ (cm/s)	4.85 ± 0.38	6.31 ± 0.58
$K(t = 230\ d)^a$ (cm/s)	4.55 ± 0.99	6.01 ± 0.21

[a] Measured.

The average wastewater flow rates were 120 and 104 L/d in FAMs 1 and 2, respectively. Because the void volume of the packed section of the FAM was 3.24 L, the hydraulic retention times (HRTs) in FAMs 1 and 2 were estimated to be 0.65 and 0.75 h, respectively. Taking into account the two unpacked sections of the FAM (clear wells), the resulting void volume was 11.24 L, and the corresponding HRTs were 2.25 and 2.59 h for FAMs 1 and 2, respectively.

The somatic coliphage levels were determined by double agar layer EPA Method 1601 (*36*). The mutant strain of *Escherichia coli* C, ATCC No. 13706 (*E. coli*), which is nalidixic acid resistant, was used as the host strain stock culture (i.e., host bacteria). Sulfite-reducing clostridium spores (CSs) were determined by inoculating the sample with a sulfite polymixin sulfadiazine agar (SPS) medium using the tube inclusion technique (*37*). For the detection and enumeration of enterococci, the water sample was filtered through a 0.45 μm membrane with a 47 mm diameter that retains bacteria. Following filtration, the membrane was placed on the surface of selective Slanetz and Bartley agar medium and incubated at 36 ± 1 °C for 44 ± 4 h. The filter was then transferred to a differential bile esculine azide agar medium and incubated at 43 ± 1 °C for 2 h (*38*). Total and fecal coliform presumptive concentrations were determined in the form of the most

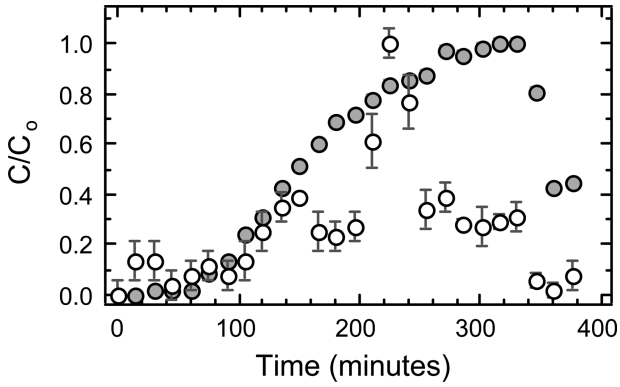

FIGURE 2. Breakthrough concentrations of the conservative tracer (electrical conductivity, solid circles) and viable somatic coliphages (open circles).

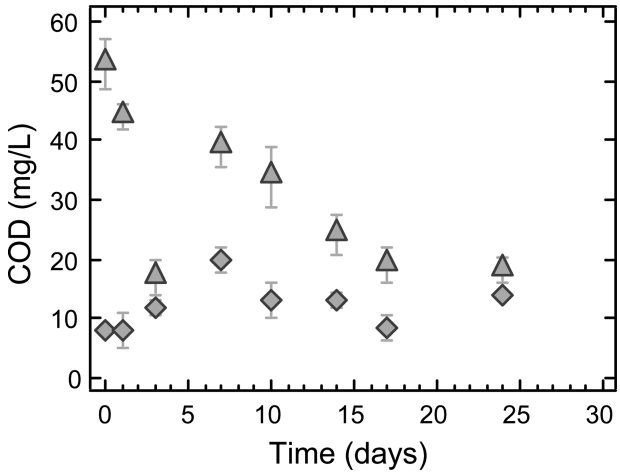

FIGURE 3. Observed effluent COD concentrations at FAM 1 (triangles) and FAM 2 (tilted squares).

probable number (MPN) by the multiple tube fermentation technique at 37 °C, using a lactose broth for a 48 h period. The total coliform confirmation test was conducted with brilliant green bile broth at 37 °C for a 24 h period. Fecal coliform confirmation tests were determined with *E. coli* broth (EC broth—CM0853, Oxoid) at 44 °C for a 24−48 h period (*35*). The *E. coli* were confirmed with the indole test in tryptone water (*39*). Total bacteria counts were determined with the pour plate method as outlined by APHA Standard Methods procedures (*35*). Two series of dishes were prepared by mixing test volumes of the water samples with molten plate count agar on Petri dishes. The number of colonies developed on the first series of dishes was counted after incubation for 44 h at 36 °C and on the second series of dishes after 72 h at 22 °C.

4. Phenomenological Clogging Model

Numerous investigators have presented mathematical models to describe clogging in granular porous media (*9, 40−42*). Here we develop a simple mathematical model for physical clogging in fractured limestone aquifers caused by biocolloid deposition. The fractured medium is represented by a set of parallel fractures with variable apertures. Assuming that the flow rate through the fractures, Q_w (L^3/t), is constant and any reduction in the time-dependent concentration of suspended biocolloids (viable plus inactivated), C (M/L^3), is due to physical sorption of biocolloids onto the fracture surfaces, the mass of the deposited biocolloids (viable plus inactivated) is given by

$$\rho_b V_{sb}(t) = Q_w t \Delta C = Q_w t[C_o - C(t)] \quad (1)$$

where ρ_b (M/L^3) is the density of the biocolloids, V_{sb} (L^3) is the time-dependent volume of the deposited biocolloids, and C_o (M/L^3) is the initial concentration of suspended biocolloids (viable plus inactivated). The volume of solids deposited onto the fracture surfaces leads to a reduction in fracture apertures and, consequently, to a reduction in porosity. The initial porosity, n_{e_o}, of a fractured formation containing parallel fractures with spatially variable aperture is given by (*6*)

$$n_{e_o} = \frac{1}{B}\sum_{i=1}^{N_f} \hat{b}_i = \frac{N_f}{B}\bar{b} \quad (2)$$

where $\hat{b}_i$ (L) is the mean aperture of fracture i, N_f (dimensionless) is the number of parallel fractures of the medium, B (L) is the thickness of the formation, and $\bar{b} = (\hat{b}_1 + \hat{b}_2 + \ldots + \hat{b}_{N_f})/N_f$ is the average of the mean apertures of the fractures. The clogged fraction of the formation porosity can be defined as

$$f_c = \frac{n_c}{n_{e_o}} \quad (3)$$

where n_c is the fraction of total volume occupied by deposited biocolloids defined as

$$n_c = \frac{V_{sb}}{V_t} = \frac{V_{sb}}{S_f B} \quad (4)$$

where V_t (L^3) is the total volume of the fractured formation and S_f (L^2) is the surface area of the fractured formation, which, for the case of horizontal and parallel fractures, is equal to the plane area of a single fracture. Combining eqs 1−4 yields an expression for the time-dependent clogged fraction of the formation porosity:

$$f_c(t) = \frac{Q_w t[C_o - C(t)]}{S_f \rho_b N_f \bar{b}} \quad (5)$$

The hydraulic conductivity, K (L/t), of a fractured formation can be obtained from Darcy's law (*6, 43*):

$$K = -\frac{Q_w}{A_f}\frac{\Delta x}{\Delta \phi} = \frac{\bar{b}^2}{12}\frac{\gamma_w}{\mu_w} n_e \quad (6)$$

where A_f (L^2) is the cross-sectional area of the fractured formation perpendicular to the flow, $\Delta\phi/\Delta x$ is the piezometric head gradient (dimensionless), γ_w [$M/(L^2 \cdot t^2)$] is the specific weight of water, and μ_w [$M/(L \cdot t)$] is the dynamic viscosity of water. For the fractured systems examined here, $n_e(t) = [1 - f_c(t)]n_{e_o}$ and consequently, $K(t)$ changes with time. Therefore, the above expression can be modified as

$$K(t) = \frac{\bar{b}^2}{12}\frac{\gamma_w}{\mu_w}[1 - f_c(t)]n_{e_o} \quad (7)$$

Substituting eq 5 into eq 7 yields the desired expression for the time-dependent hydraulic conductivity of the fractured formation:

$$K(t) = \frac{\bar{b}^2}{12}\frac{\gamma_w}{\mu_w}\left[1 - \frac{Q_w t[C_o - C(t)]}{S_f \rho_b N_f \bar{b}}\right] n_{e_o} \quad (8)$$

It should be noted that the preceding equation implicitly accounts only for physical clogging caused by suspended viable and inactivated biocolloid retention.

5. Preliminary Experiments

To simulate the field conditions of the Nardò aquifer in southern Italy where the fractures are not clean, large

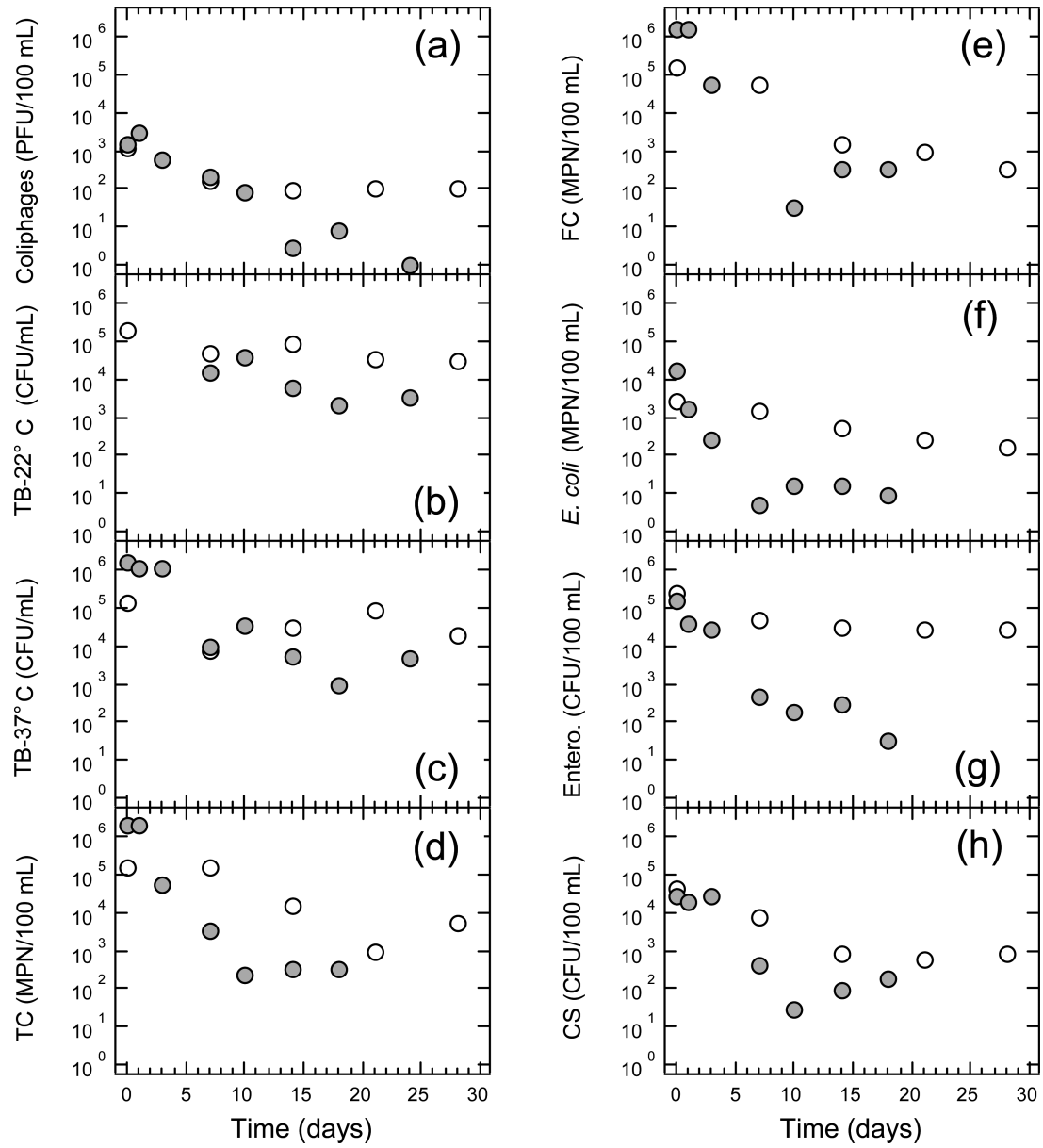

FIGURE 4. FAM 1 effluent (solid circles) and blank (open circles) concentrations for viable (a) somatic coliphages, (b) total bacterial count, TB, at 22 °C, (c) total bacterial count, TB, at 37 °C, (d) total coliforms, TCs, (e) fecal coliforms, FCs, (f) *E. coli*, (g) enterococci, and (h) sulfite-reducing clostridium spores, CSs.

quantities of reclaimed wastewater were passed through the FAMs prior to the initiation of the experiments. Furthermore, to test the pilot-scale FAM design with the terra rossa soil in place, a preliminary flow-through experiment was carried out in FAM 2. A flow line continuously (without recirculation) supplied the FAM with pretreated secondary effluent at 160 mL/min. A wastewater mixture with an EC of 1.34 mS/cm, somatic coliphages at 140 PFU/mL, and pH 7.0 was injected as a 345 min broad pulse directly into the flow line with a 30 mL/min flow rate. Due to mixing, the initial EC and concentration of somatic coliphages entering the FAM were measured as 0.58 mS/cm and 26 PFU/mL, respectively. The EC was considered a conservative tracer, and the somatic coliphages were considered a nonconservative tracer. Effluent water samples were collected every 10 min. The EC and count of somatic coliphages were measured in each sample. The experimental breakthrough data are shown in Figure 2. Note that EC recovery was at 100%, but a substantial fraction of the somatic coliphages were removed from the fluid. Note that the peak in the breakthrough of somatic coliphages, which is observed in Figure 2, is caused by detachment of previously retained biomass due to hydrodynamically induced frictional effects, which are different from those in porous media due to higher shear stress (*44, 45*). This is similar to sloughing events that take place in biologically clogged subsurface formations (*46*).

To determine the average aperture of the parallel fractures, $\bar{b}$, of the two FAMs, several flow experiments were conducted by pumping secondary wastewater effluent at various flow rates. For each flow rate, the piezometric head difference between the influent and effluent clear wells was measured, and the corresponding K was determined using eq 6. The mean K values for FAM 1 and FAM 2 were 4.85 ± 0.38 and 6.31 ± 0.38 cm/s, respectively, where the source of error is the pressure probe. The mean K values were substituted in eq 6 with $\mu_w/\gamma_w = 1.1 \times 10^{-7}$ m·s and $n_e = 4.5\%$ to obtain $\bar{b} = 1.08$ mm for FAM 1 and $\bar{b} = 1.23$ mm for FAM 2.

6. Results and Discussion

The COD provides an immediate quantitative estimate of the formation capability to degrade organic contaminants

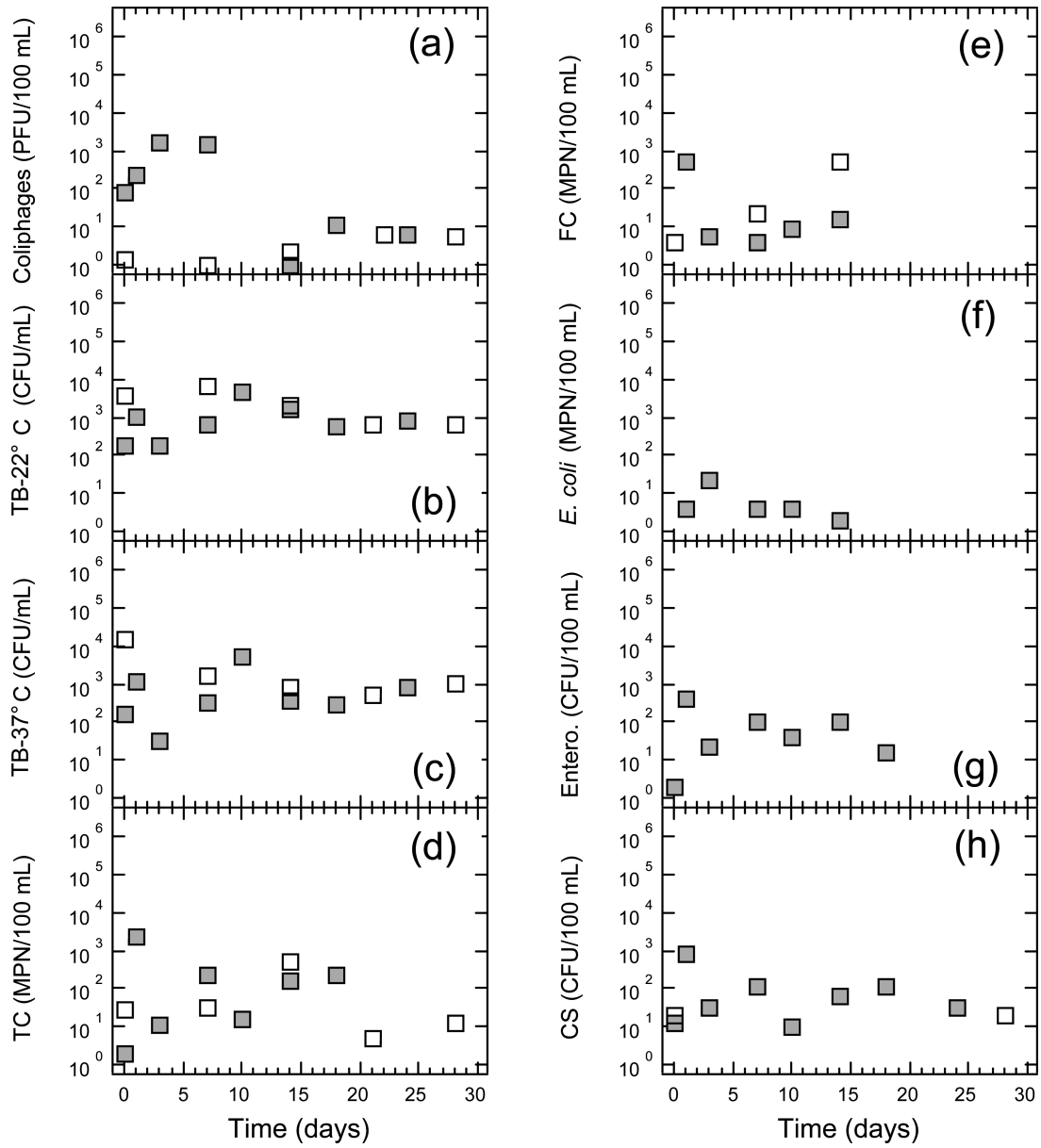

FIGURE 5. FAM 2 effluent (solid squares) and blank (open squares) concentrations for viable (a) somatic coliphages, (b) total bacterial count, TB, at 22 °C, (c) total bacterial count, TB, at 37 °C, (d) total coliforms, TCs, (e) fecal coliforms, FCs, (f) *E. coli*, (g) enterococci, and (h) sulfite-reducing clostridium spores, CSs.

in raw water through naturally occurring biochemical processes. COD enhances the heterotrophic growth of bacteria (*47, 48*). In this study, the initial COD concentration of the reclaimed wastewater used in FAM 1 was 56 mg/L, and that of the membrane reactor wastewater used in FAM 2 was 8 mg/L. The measured effluent COD concentrations for the two FAMs are shown in Figure 3. The data indicate that the COD in the effluent from FAM 1 decreased gradually from 56 to 20 mg/L and in the effluent from FAM 2 fluctuated between 8 and 20 mg/L. Although the COD was reduced by 60% in FAM 1, the COD in FAM 2 was higher in the effluent than the influent. This unusual behavior was attributed to the low concentration of pathogens entering FAM 2. Even minimal resuspension of previously retained biomass influenced the COD in the FAM effluent.

Effluent concentrations of viable pathogens were measured over a 30 d period. The experimental data are presented in Figures 4 and 5 for FAM 1 and FAM 2, respectively, together with the corresponding concentrations in the blank vessels. Comparison of the pathogen concentrations in the two blank vessels suggests that the membrane reactor effluent, which was injected into FAM 2, contained significantly lower concentrations of pathogens than the secondary effluent, which was injected into FAM 1. Note that the concentrations dropping with time in the blank vessels indicate the various pathogens undergo mild inactivation or die off. Furthermore, fecal coliforms, *E. coli*, and enterococci were initially absent from the wastewater injected into FAM 2.

Figure 4 shows that, in the effluent from FAM 1, all viable pathogen concentrations gradually decreased with time. The differences between the effluent and blank concentrations are proportional to the mass of viable pathogens retained by the FAM. Figure 5 shows that, during the early stages of the experiment, the somatic coliphage concentrations in the effluent from FAM 2 were at considerably higher levels than those in the blank vessel. Also, *E. coli* and enterococci, which were not present in the influent, were detected in the effluent. These discrepancies were attributed to the detachment of previously deposited biocolloids, which were retained by FAM 2 during earlier FAM operations with reclaimed wastewater. It should be noted that inactivated biocolloids, which have been deposited/attached onto the soil and fracture surfaces

of the FAMs, could not be estimated from the experimental data presented in Figures 4 and 5. However, both viable and inactivated biocolloids contributed to K reduction of the FAMs.

The pathogen removal shown in Figures 4 and 5 is in agreement with field observations at the Nardò fractured aquifer where significant pathogen removal was observed (*6*). However, it should be noted that Brownian motion of biocolloid particles migrating in a fracture generates movement of particles in a direction normal to the flow (*49*) that leads to particle exclusion from the slowest streamlines closest to the wall, which in turn reduces the probability of biocolloid attachment onto fracture walls. Biocolloid transport and attachment onto fracture wall surfaces are not independent processes and can be significantly affected by the water chemistry, the temperature, and biocolloid inactivation (*5, 13, 15, 17, 50*). Biocolloid attachment onto fracture wall surfaces is mainly dominated by repulsive electrostatic, attractive van der Waals, and hydrodynamic forces; also, biocolloid deposition is often characterized by either equilibrium or kinetic relationships (*26, 27, 51*). Although the two FAMs employed in this study were designed to simulate as close as possible the conditions at the Nardò fractured aquifer, there are a few very distinct differences between the laboratory and field scales and conditions that can affect biocolloid transport and retention. At the Nardò fractured aquifer the reservoir geometry is far more complex than that of the FAM used in this study. At the Nardò aquifer the fractures are not perfectly horizontal; instead they construct a fracture network structure with intersecting fractures that form various bifurcations (*6, 52*) where buoyant biocolloids partition between daughter fractures in proportion to flow rates and dense biocolloids preferentially exit fractures that are gravitationally downgradient (*53*). Furthermore, pathogen inactivation appears to be faster in the field than in the laboratory. This difference may be attributed to several factors including the water chemistry and temperature, as well as the extent of pre-existing biomass accumulation onto fracture wall surfaces. Note that artificial recharge with secondary municipal effluents at the Nardò fractured aquifer was initiated in 1991 (*30*).

Both FAMs were operated well beyond the 30 d period of the viable pathogen measurements presented in Figures 4 and 5. After 230 d of operation, the K values of FAMs 1 and 2 were measured again. Both FAMs showed decreased hydraulic conductivity over the 230 d period. The K of FAM 1 was reduced from 4.85 to 4.55 cm/s (6.2% reduction) and that of FAM 2 from 6.31 to 6.01 cm/s (4.8% reduction). The K reduction was more pronounced in FAM 1 than in FAM 2 because FAM 1 was supplied with secondary effluent containing higher concentration of organics and pathogens than the membrane reactor effluent of FAM 2. Therefore, there were more biocolloids available in FAM 1. Note that the COD in FAM 1 was higher than in FAM 2 (see Figure 3). After the completion of the experiments the FAMs were dismantled. Inspection of the limestone plates indicated that a few biocolloids migrated into the pores of the limestone, probably at the early stages of the experiment, and the majority of the biocolloids accumulated onto the fracture surfaces.

Assuming that the observed K reduction was caused solely by biocolloid retention, the mass of biocolloids retained by the two FAMs over the 230 d period can be estimated. Using the parameters $S_f = 3600$ cm^2, $n_e = 4.5\%$, $\mu_w/\gamma_w = 1.1 \times 10^{-7}$ m·s, $N_f = 16$, and $t = 230$ d, eq 8 was employed with $Q_w = 120$ L/d, $\rho_b = 1.066$ g/cm^3, $\bar{b} = 1.08$ mm, and $K = 4.55$ cm/s to determine that the 6.2% reduction observed in K for FAM 1 occurs for $\Delta C = 0.204$ mg/L. Similarly, eq 8 was employed with $Q_w = 104$ L/d, $\rho_b = 1.066$ mg/cm^3, $\bar{b} = 1.23$ mm, and $K = 6.01$ cm/s to determine that the 4.8% reduction observed in the K value of FAM 2 corresponds to $\Delta C = 0.279$ mg/L. The estimated $\Delta C = C_o - C(t)$ was larger for FAM 2 because $\bar{b}$ was larger for FAM 2 (see Table 1). However, the estimated ΔC values are inflated because eq 8 assumes that the reduction in K is due only to biocolloid retention.

Acknowledgments

This research was supported in part by the EU under an INTERREG Greece-Italy research grant. We thank the three anonymous reviewers for their useful suggestions and comments, which improved the quality of this paper.

Literature Cited

(1) Levine, A. D.; Asano, T. Recovering sustainable water from wastewater. *Environ. Sci. Technol.* **2004**, *38*, 201A.
(2) Bixio, D.; Thoeye, C.; De Koning, J.; Joksimovic, D.; Savic, D.; Wintgens, T.; Melin, T. Wastewater reuse in Europe. *Desalinatio.* **2006**, *187*, 89–101.
(3) Bouwer, H. Artificial recharge of groundwater: Hydrogeology and engineering. *Hydrogeol. J.* **2002**, *10*, 121–142.
(4) Sheng, Z. An aquifer storage and recovery system with reclaimed wastewater to preserve native groundwater resources in El Paso, Texas. *J. Environ. Manage.* **2005**, *75*, 367–377.
(5) Anders, R.; Chrysikopoulos, C. V. Evaluation of factors controlling the time-dependent inactivation rate coefficients of bacteriophage MS2 and PRD1. *Environ. Sci. Technol.* **2006**, *40*, 3237–3242.
(6) Masciopinto, C.; La Mantia, R.; Chrysikopoulos, C. V. Fate and transport of pathogens in a fractured aquifer in the Salento area, Italy. *Water Resour. Res.* **2008**, *44*, W01404.
(7) Anders, R.; Chrysikopoulos, C. V. Virus fate and transport during artificial recharge with recycled water. *Water Resour. Res.* **2005**, *41* (10), W10415.
(8) Rinck-Pfeiffer, S.; Ragusa, S.; Sztajnbok, P.; Vandevelde, T. Interrelationships between biological, chemical, and physical processes as an analog to clogging in aquifer storage (ASR) wells. *Water Res.* **2000**, *34*, 2110–2118.
(9) Pavelic, P.; Dilon, P. J.; Barry, K. E.; Vanderzalm, J. L.; Correll, R. L.; Rinck-Pfeiffer, M. Water quality effects on clogging rates during reclaimed water ASR in a carbonate aquifer. *J. Hydrol.* **2007**, *334*, 1–16.
(10) Chrysikopoulos, C. V.; Sim, Y. One-dimensional virus transport in homogeneous porous media with time dependent distribution coefficient. *J. Hydrol.* **1996**, *185*, 199–219.
(11) Sim, Y.; Chrysikopoulos, C. V. One-dimensional virus transport in porous media with time dependent inactivation rate coefficients. *Water Resour. Res.* **1996**, *32* (8), 2607–2611.
(12) Redman, J. A.; Grant, S. B.; Olson, T. M.; Estes, M. K. Pathogen filtration, heterogeneity, and the potable reuse of wastewater. *Environ. Sci. Technol.* **2001**, *35*, 1798–1805.
(13) Harvey, R. W.; Ryan, J. N. Use of PRD1 bacteriophage in groundwater viral transport, inactivation, and attachment studies. *FEMS Microbiol. Ecol.* **2004**, *49*, 3–16.
(14) Anders, R.; Chrysikopoulos, C. V. Transport of viruses through saturated and unsaturated columns packed with sand. *Transp. Porous Media* **2009**, *76*, 121–138.
(15) Bales, R. C.; Hinkle, S. R.; Kroeger, T. W.; Stocking, K.; Gerba, C. P. Bacteriophage adsorption during transport through porous media: Chemical perturbations and reversibility. *Environ. Sci. Technol.* **1991**, *25*, 2088–2095.
(16) Cheng, L.; Chetochine, A. S.; Pepper, I. L.; Brusseau, M. L. Influence of DOC on MS-2 bacteriophage transport in a sandy soil. *Water, Air, Soil Pollut.* **2007**, *178*, 315–322.
(17) Yates, M. V.; Yates, S. R.; Wagner, J.; Gerba, C. P. Modeling virus survival and transport in the subsurface. *J. Contam. Hydrol.* **1987**, *1*, 329–345.
(18) Sim, Y.; Chrysikopoulos, C. V. Virus transport in unsaturated porous media. *Water Resour. Res.* **2000**, *36* (1), 173–179.
(19) Chu, Y.; Jin, Y.; Flury, M.; Yates, M. V. Mechanisms of virus removal during transport in unsaturated porous media. *Water Resour. Res* **2001**, *37* (2), 253–263.
(20) Ross, N.; Villemur, R.; Deschenes, L.; Samson, R. Clogging of a limestone fractured by stimulating groundwater microbes. *Water Res.* **2001**, *35* (8), 2029–2037.
(21) Arnon, S.; Adar, E.; Ronen, Z.; Yakirevich, A.; Nativ, R. Impact of microbial activity on the hydraulic properties of fractured chalk. *J. Contam. Hydrol.* **2005**, *76*, 315–336.

(22) Oberdorfer, J. A.; Peterson, F. L. Waste-water injection: geochemical and biochemical clogging processes. *Ground Water* **1985**, *23* (6), 753–761.
(23) Baveye, P.; Vandevivere, P.; Hoyle, B. L.; DeLeo, P. C.; de Lozada, D. S. Environmental impact and mechanisms of the biological clogging of saturated soils and aquifer materials. *Crit. Rev. Environ. Sci. Technol.* **1998**, *28*, 123–191.
(24) Singurindy, O.; Berkowitz, B. The role of fractures on coupled dissolution and precipitation patterns in carbonate rocks. *Adv. Water Resour.* **2005**, *28*, 507–521.
(25) James, S. C.; Bilezikjian, T. K.; Chrysikopoulos, C. V. Contaminant transport in a fracture with spatially variable aperture in the presence of monodisperse and polydisperse colloids. *Stochastic Environ. Res. Risk Assess.* **2005**, *19* (4), 266–279.
(26) Gerba, C. P.; Keswick, B. H. Survival and transport of enteric bacteria and viruses in groundwater. *Stud. Environ. Sci.* **1981**, *17*, 511–515.
(27) Chrysikopoulos, C. V.; Abdel-Salam, A. Modeling colloid transport and deposition in saturated fractures. *Colloids Surf., A* **1997**, *121*, 189–202.
(28) Vandevivere, P.; Baveye, P.; de Lozada, D. S.; DeLeo, P. Microbial clogging of saturated soils and aquifer materials: Evaluation of mathematical models. *Water Resour. Res.* **1995**, *31*, 2173–2180.
(29) Mays, D. C.; Hunt, J. R. Hydrodynamic aspects of particle clogging in porous media. *Environ. Sci. Technol.* **2005**, *39*, 577–584.
(30) Masciopinto, C.; Carrieri, C. Assessment of water quality after 10 years of reclaimed water injection: The Nardò fractured aquifer (Southern Italy). *Ground Water Monit. Rem.* **2002**, *22* (1), 88–97.
(31) Dell'Anna, L.; Fiore, S.; Laviano, R. The mineralogical, chemical and grain-size features of some dry deposits from terra rossa d'Otranto (Puglia, Southern Italy). *Geol. Appl. Idrogeol.* **1985**, *20* (1), 110–123.
(32) Chrysikopoulos, C. V.; Roberts, P. V.; Kitanidis, P. K. One-dimensional solute transport in porous media with partial well-to-well recirculation: Application to field experiments. *Water Resour. Res.* **1990**, *26* (6), 1189–1195.
(33) Narayan, R.; Coury, J. R.; Masliyah, J. H.; Gray, M. R. Particle capture and plugging in packed-bed reactors. *Ind. Eng. Chem. Res.* **1997**, *36*, 4620–4627.
(34) Dowd, S. E.; Pillai, S. D.; Wang, S.; Corapcioglu, M. Y. Delineating the specific influence of virus isoelectric point and size on virus adsorption and transport through sandy soil. *Appl. Environ. Microbiol.* **1998**, *64* (2), 405–410.
(35) Clesceri, L. S., Greenberg, A. E., Eaton, A. D., Eds. *Standard Methods for the Examination of Water and Wastewater*, 20th ed., American Public Health Association: Washington, DC, 1998.
(36) U.S. EPA. *Method 1601: Male-Specific (F+) and Somatic Coliphage in Water by Two-Step Enrichment Procedure*; EPA-821-R-01−030; Washington, DC, 2001.
(37) ISTISAN (Istituto Superiore di Sanità). *Report 02/8: Clostridium perfringens as an Environmental Pollution Indicator and Its Hygienic Role*; Rome, Italy, 2002; pp 16−20.
(38) *Water Quality. Detection and Enumeration of Intestinal Enterococci. Part 2: Membrane Filtration Method*; SFS-EN ISO 7899-2; Finnish Standards Association: Helsinki, Finland, 2000.
(39) U.K. Environment Agency. *Methods for the Examination of Waters and Associated Materials. The Microbiology of Drinking Water—Part 4: Methods for the Isolation and Enumeration of Coliform Bacteria and Escherichia coli (Including E. coli O157: H7)*; Bristol, U.K., 2002.
(40) Blazejewski, R.; Murat-Blazejewska, S. Soil clogging phenomena in constructed wetlands with subsurface flow. *Water Sci. Technol.* **1997**, *35* (5), 183–188.
(41) Perez-Paricio, A. Integrated modelling of clogging processes in artificial groundwater recharge. Ph.D. Thesis, Department of Geotechnical Engineering and GeoSciences, Technical University of Catalonia, Barcelona, Spain, 2001.
(42) Skolasinska, K. Clogging microstructures in the vadose zone—Laboratory and field studies. *Hydrogeol. J.* **2006**, *14* (6), 1005–1017.
(43) Bear, J. Modeling flow and contaminant transport in fractured rocks. In *Flow and Contaminant Transport in Fractured Rock*; Bear, J., Tsang, C. F., de Marsily, G., Eds.; Academic Press: San Diego, CA, 1993; Chapter 1, pp 67−272.
(44) Khilar, K. C.; Fogler, H. S. *Migration of Fines in Porous Media*; Kluwer: Dordrecht, The Netherlands, 1998.
(45) Dupin, H. J.; McCarty, P. L. Impact of colony morphologies and disinfection on biological clogging in porous media. *Environ. Sci. Technol.* **2000**, *34*, 1513–1520.
(46) Peyton, B. M.; Characklis, W. G. A statistical analysis of the effect of substrate utilization and shear stress on the kinetics of biofilm detachment. *Biotechnol. Bioeng.* **1993**, *41*, 728–735.
(47) Leverenz, H. L.; Tchobanoglous, G.; Darby, J. L. Clogging in intermittently dosed sand filters used for wastewater treatment. *Water Res.* **2009**, *43* (3), 695–705.
(48) Garcia, J.; Rousseau, D.; Caselles-Osorio, A.; Story, A.; De Pauw, N.; Vanrollenghem, P. Impact of prior physico-chemical treatment on the clogging process of subsurface flow constructed wetlands: Model-based evaluation. *Water, Air, Soil Pollut.* **2007**, *185*, 101–109.
(49) James, S. C.; Chrysikopoulos, C. V. Effective velocity and effective dispersion coefficient for finite-sized particles flowing in a uniform fracture. *J. Colloid Interface Sci.* **2003**, *263*, 288–295.
(50) Abdel-Salam, S. C.; Chrysikopoulos, C. V. Analytical solutions for one-dimensional colloid transport in saturated fractures. *Adv. Water Resour.* **1994**, *17* (5), 283–296.
(51) James, S. C.; Chrysikopoulos, C. V. Analytical solutions for monodisperse and polydisperse colloid transport in uniform fractures. *Colloids Surf., A* **2003**, *226*, 101–118.
(52) Berkowitz, B. Characterizing flow and transport in fractured geological media: A review. *Adv. Water Resour.* **2002**, *25*, 861–884.
(53) James, S. C.; Chrysikopoulos, C. V. Dense colloid transport in a bifurcating fracture. *J. Colloid Interface Sci.* **2004**, *270*, 250–254.

ES902754N